NRL Memorandum Report 4441

# Stability Properties of Azimuthally Symmetric Perturbations in an Intense Electron Beam

HAN S. UHM

*Naval Surface Weapons Center*
*White Oak, Silver Spring, Md. 20910*

MARTIN LAMPE

*Plasma Theory Branch*
*Plasma Physics Division*



February 3, 1981

Sponsored by
Defense Advanced Research Projects Agency (DOD)
ARPA Order No. 3718
Monitored by C.M. Huddleston Under Contract #N60921-80-WR-W0190



NAVAL RESEARCH LABORATORY
Washington, D.C.

(9) Memorandum report

SECURITY CLASSIFICATION OF THIS PAGE (When Data Entered)

| REPORT DOCUMENTATION PAGE | | READ INSTRUCTIONS BEFORE COMPLETING FORM |
|---|---|---|
| 1. REPORT NUMBER (14) NRL-MR- NRL Memorandum Report 4441 | 2. GOVT ACCESSION NO. AD-A094 | 3. RECIPIENT'S CATALOG NUMBER 535 |
| 4. TITLE (and Subtitle) (6) STABILITY PROPERTIES OF AZIMUTHALLY SYMMETRIC PERTURBATIONS IN AN INTENSE ELECTRON BEAM, | | 5. TYPE OF REPORT & PERIOD COVERED Interim report on a continuing NRL problem. |
| | | 6. PERFORMING ORG. REPORT NUMBER |
| 7. AUTHOR(s) (10) Han S. Uhm* and Martin Lampe | (11) 3 Feb 81 | 8. CONTRACT OR GRANT NUMBER(s) |
| 9. PERFORMING ORGANIZATION NAME AND ADDRESS Naval Research Laboratory Washington, D.C. 20375 (12) 50 | (15) VV | 10. PROGRAM ELEMENT, PROJECT, TASK AREA & WORK UNIT NUMBERS ARPA Order No. 3718; Source Code: 11012, #N60921-80-WR-W0190; 47-0900-0-1 |
| 11. CONTROLLING OFFICE NAME AND ADDRESS Defense Advanced Research Projects Agency Arlington, VA 22209 | | 12. REPORT DATE February 3, 1981 |
| | | 13. NUMBER OF PAGES 49 |
| 14. MONITORING AGENCY NAME & ADDRESS(if different from Controlling Office) | | 15. SECURITY CLASS. (of this report) UNCLASSIFIED |
| | | 15a. DECLASSIFICATION/DOWNGRADING SCHEDULE |

16. DISTRIBUTION STATEMENT (of this Report)

Approved for public release; distribution unlimited.

17. DISTRIBUTION STATEMENT (of the abstract entered in Block 20, if different from Report)

18. SUPPLEMENTARY NOTES

This report was sponsored by Defense Advanced Research Projects Agency (DOD) ARPA Order No. 3718
Monitored by C. M. Huddleston under Contract #N60921-80-WR-W0190
*Naval Surface Weapons Center, White Oak, Silver Spring, MD 20910

19. KEY WORDS (Continue on reverse side if necessary and identify by block number)

Beam propagation
Heavy ion fusion
Hose instability
Sausage instability
Hollowing instability

20. ABSTRACT (Continue on reverse side if necessary and identify by block number)

The Vlasov-Maxwell equations are used to investigate the stability of azimuthally symmetric perturbations (e.g., sausage and hollowing modes) of an electron or ion beam immersed in a resistive plasma. The perturbed space charge and plasma current are treated self-consistently for any value of the plasma conductivity. A similar analysis of the hose instability is also carried out. It is assumed that $\nu/\gamma_b << 1$, where $\nu$ is Budker's parameter and $\gamma_b mc^2$ is the characteristic beam electron energy. The analysis is carried out for the "loss-cone" distribution function in which all of the beam electrons have the same value of energy (in a frame of reference rotating with angular velocity $\omega_b$) and the same value of axial canonical momentum. In the high conductivity regime, the system is shown to be strongly destabilized by a sufficiently large value of the fractional current neutralization.

DD FORM 1 JAN 73 1473 EDITION OF 1 NOV 65 IS OBSOLETE S/N 0102-LF-014-6601



SECURITY CLASSIFICATION OF THIS PAGE (When Data Entered)

251950

CONTENTS



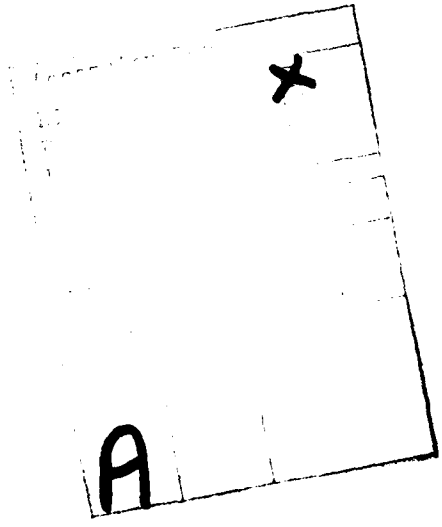

# STABILITY PROPERTIES OF AZIMUTHALLY SYMMETRIC PERTURBATIONS IN AN INTENSE ELECTRON BEAM

## I. INTRODUCTION

In recent years there have been numerous theoretical investigations of the equilibrium[1,2] and stability[3-8] properties of intense charged particle beams, motivated by a variety of applications, including confinement and transport[9-11] of a nonneutral electron beam, inertial confinement fusion[12,13] driven by charged particle beams, and electron beam propagation[14,15] through a background plasma. Although these research activities have different goals and objectives, they have in common the need to understand the stability properties of intense charged beams characterized by strong self electric and magnetic fields. However, previous theoretical studies of the resistive instabilities (except for hose) have been based on highly simplified models, such as the cold fluid treatment of Ref. 8. The primary purpose of the present paper is to develop a Vlasov-Maxwell description of azimuthally symmetric perturbations about an electron beam, including the higher radial mode numbers (e.g. hollowing modes), which have been given scant attention in the literature, although they appear to be troublesome in the presence of a return current. We also include a treatment of the hose instability based on the same model. With straightforward modifications, the results of this paper can also be applied to the transverse instabilities[12,16,17] of an intense ion beam, which are particularly important in heavy-ion fusion applications.

The equilibrium and stability analysis is carried out for an infinitely long electron beam propagating parallel to a uniform applied magnetic field $B_0\hat{e}_z$ through a background plasma with conductivity $\sigma(r)$, which in general can be a function of the oscillation frequencies of fluctuating fields and the collision frequencies of each species in the

Manuscript submitted December 1, 1980.

plasma. Our solutions are carried out for step-function profiles and real values of $\sigma(r)$, but the value of $\sigma$ can be arbitrarily large or small. The radial profiles of plasma charge and current are assumed to be similar to the beam profile, but the degree of charge and current neutralization is arbitrary. It is assumed that $\nu/\gamma_b << 1$, where $\nu$ and $\gamma_b mc^2$ are Budker's parameter and the characteristic energy, respectively, m is the electron rest mass and c is the speed of light in vacuo. Equilibrium and stability properties are calculated for an electron beam described by a "loss-cone" distribution function [Eq. (2)], which leads to a flat-topped beam radial profile. Equilibrium properties and basic assumptions are briefly discussed in Sec. II.

The formal stability analysis for azimuthally symmetric perturbations is carried out in Sec. III, within the framework of the linearized Vlasov-Maxwell equations. In the analysis, the response of the background plasma is incorporated in terms of the plasma conductivity. An integro-differential eigenvalue equation [Eqs. (22)] is obtained for azimuthally symmetric perturbations, given any value of plasma conductivity, assuming long wavelength ($kR_b << 1$), low frequency ($\omega R_b << c$) perturbations, where k is the axial wavenumber, $\omega$ is the oscillation frequency, and $R_b$ is the beam radius. Equations (22) constitute a principal result of this paper and can be used to investigate stability properties for a broad range of system parameters.

In Sec. IV, dispersion relations for the radial mode numbers n = 0, 1 and 2 are obtained analytically from the integro-differential eigenvalue equation (22) by an approximation method based on the assumption $\omega\tau_d \lesssim 1$,

where $\tau_d$ is a magnetic decay time defined by $\tau_d = \pi\hat{\sigma}_1 R_b^2/2c^2$ [Eq. (26)]. For example, the dispersion relation for the n = 1 (sausage) mode can be expressed as [Eq. (65)],

$$Z^2 - \eta + \frac{\zeta\beta_b^2 + i/\gamma_b^2}{(\zeta - i)\left[1 - i\zeta(\omega R_b/c)^2/6\right]} = 0,$$

where $Z = (\omega - k\beta_b c)/\hat{\omega}_{pb}$ is the normalized Doppler-shifted eigenfrequency, $\eta \equiv 2[\beta_b^2(1 - f_m) - (1 - f_e)] + \omega_{cb}^2/\hat{\omega}_{pb}^2$ and $\zeta \equiv 4\pi\hat{\sigma}_1/\omega$ are the focussing force and conductivity parameters, respectively, $\beta_b^2 = (\gamma_b^2 - 1)/\gamma_b^2$, $\omega_{cb} = eB_0/\gamma_b mc$ and $\hat{\omega}_{pb} = (4\pi e^2\hat{n}_b/\gamma_b m)^{1/2}$ are the beam electron cyclotron and plasma frequencies, respectively, $f_e$ and $f_m$ are the fractional charge and current neutralization, respectively. The limiting case of a non-neutral electron beam in a non-conducting environment ($\zeta \to 0$) is discussed in Sec. IV. For example, in the limit of $\zeta = 0$, the dispersion relation for n = 1 [in Eq. (65)] reduces to

$$Z^2 = \eta + 1/\gamma_b^2 ,$$

which is identical to the previous result obtained by Uhm and Davidson.[3]

Analytic investigations of the dispersion relations for n = 0, 1 and 2 are carried out in Sec. V.A for collision-dominated plasmas with a high conductivity satisfying $\zeta >> 1$. We find that both the n = 1 (sausage) and n = 2 (hollowing) modes are driven unstable by either a strong fractional plasma return current ($f_m$) or by a magnetic phase lag ($\omega\tau_d > 0$). As an example a simplified version of the n = 1 dispersion relation [Eq. (67)],

$$Z^2 = \beta_b^2\left[(1 - 2f_m) - \frac{i\zeta}{6}(\omega R_b/c)^2\right] ,$$

which is obtained from Eq. (65) in the limit of $\eta = 2\beta_b^2(1 - f_m)$ and $\omega\tau_d << 1$, shows clearly that the system is unstable whenever the fractional current neutralization $f_m > 0.5$, even for a very small magnetic decay time. It is also remarkable to observe that for $f_m = 0$, Eq. (67) is similar to the result obtained by Weinberg[8] within the framework of the coaxial circular orbit beam model.

Several points are noteworthy in the numerical analysis of the dispersion relations presented in Sec. V.B. for a self-pinched electron beam ($\omega_{cb} = 0$). First, the n = 1 perturbation is the most unstable azimuthally symmetric mode. Even if $f_m = 0$, the maximum growth rate of instability for the n = 1 perturbation is $Z_i = \mathrm{Im}Z = 0.205$, which is comparable to that of the resistive hose instability.[7] Second, the n = 2 perturbation has two unstable modes. Third, except the n = 0 perturbation, we find for $f_m = 0$ that the growth rate of instability goes through two maxima as $\zeta$ is varied. The first maximum occurs at $\zeta \simeq 1$, where electrostatic effects are strong, and the second one at $\omega\tau_d \simeq 1$ where the instability is driven by the magnetic phase lag. For a highly relativistic beam, the growth rate is equal at the two maxima.

In Sec. VI, similar models and analytic techniques are applied to the theory of the hose instability in a medium of arbitrary conductivity, and with arbitrary values of the fractional charge and current neutralization. The instability properties are similar in many respects to those of the m = 0 modes: the hose instability also has maximum growth rates at $\zeta \approx 1$ and $\omega\tau_d \sim 1$, it too is driven strongly unstable by return current, and the hose growth rates are comparable to those of the sausage.

## II. EQUILIBRIUM THEORY AND BASIC ASSUMPTIONS

The equilibrium configuration consists of an intense electron beam that is propagating parallel to a uniform applied magnetic field $B_0\hat{e}_z$ through a background plasma with a conductivity $\sigma(r)$, and is located inside a grounded cylindrical conducting wall with radius $R_c$. Cylindrical polar coordinates $(r,\theta,z)$ are used, with the z-axis along the axis of symmetry. In equilibrium $(\partial/\partial t = 0)$, the beam is assumed to be azimuthally symmetric $(\partial/\partial\theta = 0)$, infinitely long, and axially uniform $(\partial/\partial z = 0)$. The number of electrons per unit axial length $(N_b)$ is defined by

$$N_b = 2\pi \int_0^\infty dr\, r\, n_b^0(r) = \pi R_b^2 n_b^0(r = 0) \ ,$$

where $n_b^0(r)$ is the equilibrium density profile, and $R_b$ is the characteristic beam radius. In the present analysis, we assume that

$$\frac{\nu}{\gamma_b} = \frac{N_b e^2}{mc^2}\ \frac{1}{\gamma_b} << 1, \tag{1}$$

where $\nu$ is Budker's parameter, c is the speed of light in vacuo, $\gamma_b mc^2$ is the characteristic electron energy, -e and m are the electron charge and rest mass, respectively. Equation (1) guarantees that the beam is paraxial, i.e., transverse electron velocities are much smaller than axial velocities.

In this paper, we investigate the equilibrium and stability properties for a steady-state $(\partial/\partial t = 0)$ beam distribution of the form

$$f_b^0(H,P_\theta,P_z) = \frac{\hat{n}_b}{2\pi\gamma_b m}\ \delta(H - \omega_b P_\theta - \hat{\gamma} mc^2)\ \delta\ (P_z - \gamma_b m \beta_b c), \tag{2}$$

where the total energy, $H = (m^2c^4 + c^2\underset{\sim}{p}^2)^{\frac{1}{2}} - e\phi_0(r)$, the canonical angular momentum, $P_\theta = rp_\theta - eB_0r^2/2c$, and the axial canonical momentum, $P_z = p_z - (e/c)A_0(r)$, are the three single-particle constants of the motion in the equilibrium fields. Here, $\underset{\sim}{p} = (p_r, p_\theta, p_z)$ is the mechanical momentum, $\hat{n}_b$, $\omega_b$, and $\hat{\gamma}$ are constants, $\gamma_b$ is related to $\beta_b$ by $\gamma_b = (1 - \beta_b^2)^{-\frac{1}{2}}$, $A_0(r)$ is the axial component of vector potential for the equilibrium azimuthal self-magnetic field, and $\phi_0(r)$ is the equilibrium electrostatic potential. As a consequence of Eqs. (1) and (2), all electrons have axial velocities $v_z$ very close to the constant value $\beta_b c$.

In order to make the theoretical analysis tractable, we assume that in equilibrium the plasma space charge provides a fractional neutralization of the beam charge that is uniform through r and z, i.e.,

$$n_i^0(r) - n_e^0(r) = f_e n_b^0(r) \ , \tag{3}$$

where $f_e$ is constant with $0 \leq f_e \leq 1$. It is further assumed that the equilibrium plasma return current $J_p^0(r)$ has the same radial profile as the beam current $J_b^0(r)$, i.e.,

$$J_p^0(r) = - f_m J_b^0(r) \ ,$$

where $f_m$ is a positive constant with $0 \leq f_m \leq 1$. An eigenvalue treatment of the instability is possible only if $f_e$ and $f_m$ are taken to be z - independent (which is not strictly consistent in a resistive medium). Radial profiles of plasma charge and current which differ from the beam profile are of interest, but are not studied in the present paper.

Since the beam is paraxial, it is straightforward to show that the term $H - \omega_b P_\theta$ in Eq. (2) can be approximated by[5]

$$H - \omega_b P_\theta = \gamma_b mc^2 + \frac{p_\perp^2}{2\gamma_b m} + \psi_0(r) \quad , \tag{4}$$

where $p_\perp^2 = p_r^2 + (p_\theta - \gamma_b m\omega_b r)^2$ is the transverse momentum-squared in a rotating frame with the angular velocity $\omega_b$, and the effective potential $\psi_0(r)$ is defined by

$$\psi_0(r) = \frac{1}{2}\gamma_b m(\omega_b^+ - \omega_b)(\omega_b - \omega_b^-)r^2, \tag{5}$$

In Eq. (5),

$$\omega_b^\pm = \frac{\omega_{cb}}{2} \pm \left\{ \frac{\omega_{cb}^2}{4} + \frac{\hat{\omega}_{pb}^2}{2}[\beta_b^2(1 - f_m) - (1 - f_e)] \right\}^{1/2} , \tag{6}$$

where $\omega_{cb} = eB_0/\gamma_b mc$ is the beam electron cyclotron frequency and $\hat{\omega}_{pb}^2 = 4\pi e^2 n_b/\gamma_b m$ is the beam electron plasma frequency-squared. For radial confinement in the equilibrium state, it is required from Eq. (6) that

$$\hat{\omega}_{pb}^2\beta_b^2(1 - f_m) + \omega_{cb}^2/2 > \hat{\omega}_{pb}^2(1 - f_e) \quad , \tag{7}$$

which assures that the repulsive space-charge force on the beam electron is weaker than the magnetic focussing force.

Making use of Eqs. (2) and (4), we find the beam density profile

$$n_b^0(r) = \begin{cases} \hat{n}_b , & 0 \le r < R_b , \\ 0 , & R_b < r < R_c , \end{cases} \tag{8}$$

where the beam radius $R_b$ is defined by

$R_b^2 = 2c^2 (\hat{\gamma}\gamma_b^{-1} - 1)(\omega_b^+ - \omega_b)^{-1}(\omega_b - \omega_b^-)^{-1}$. The equilibrium solution exists

for rotational frequency satisfying $\omega_b^- < \omega_b < \omega_b^+$. Additional equilibrium properties associated with the distribution function in Eq. (2) are discussed in Refs. 3 and 5.

## III. LINEARIZED VLASOV-MAXWELL EQUATIONS

In this section, we use the linearized Vlasov-Maxwell equations to obtain an integro-differential eigenvalue equation for the azimuthally symmetric ($\partial/\partial\theta = 0$) modes of an electron beam. We adopt a normal mode approach in which all perturbed quantities are assumed to vary with z and t as

$$\tilde{\Phi}(\underset{\sim}{x},t) = \hat{\Phi}(r)\exp[\,i(kz - \omega t)\,] \ ,$$

with $\mathrm{Im}\omega > 0$. Here $\omega$ is the oscillation frequency and k is the axial wavenumber. For paraxial beams with all electron axial velocities approximately constant at $v_z = \beta_b c$ [which follows from (1) and (2)], it is more convenient to use $\tau$ and z, rather than t and z, as independent variables, where $\tau \equiv t - z/v_z$. In this representation, a Fourier decomposition of perturbed quantities is expressed as

$$\tilde{\Phi}(\underset{\sim}{x},t) = \hat{\Phi}(r)\exp[\,-i(\omega\tau + \Omega z/v_z)\,] \ , \tag{9}$$

where $\Omega \equiv \omega - kv_z = \omega - k\sigma\beta_b$ is the shifted eigenfrequency "seen" by a beam particle (but no relativistic charge of frame is implied).

The subsequent stability analysis is restricted to a long wavelength and low frequency perturbation characterized by

$$|kR_b|^2 << 1 \ , \qquad \left|\frac{\omega R_b}{c}\right|^2 << 1 \ . \tag{10}$$

If we forego the possibility of recovering the non-neutral limit, $\sigma \to 0$ , the analysis can be carried through with the weaker assumptions

$$|\Omega\, R_b/c| << 1 \tag{11}$$

and

$$\left| kR_b/\gamma_b^2 \right| << 1 \ . \tag{12}$$

Equation (11) is a weak form of "frozen field" assumption, based on the fact that $\Omega$ is characterized by the natural oscillation frequencies of particle dynamics, $\omega_b^{\pm}$ and $\omega_{pb}\beta_b$, which always satisfy (11) in a paraxial beam. Assumption (12) is satisfied either for long wavelengths or in a highly relativistic beam.

The perturbed electric and magnetic fields, $\hat{\underset{\sim}{E}}(\underset{\sim}{x})$ and $\hat{\underset{\sim}{B}}(\underset{\sim}{x})$, can be expressed in terms of perturbed magnetic and electric potentials $\hat{\underset{\sim}{A}}(\underset{\sim}{x})$ and $\hat{\phi}(\underset{\sim}{x})$:

$$\hat{\underset{\sim}{B}}(\underset{\sim}{x}) = \underset{\sim}{\nabla} \times \hat{\underset{\sim}{A}}(\underset{\sim}{x}) \ , \tag{13a}$$

$$\hat{E}(x) = i \frac{\omega}{c} \hat{\underset{\sim}{A}}(\underset{\sim}{x}) - \underset{\sim}{\nabla}\hat{\phi}(\underset{\sim}{x}) \ . \tag{13b}$$

Introducing the Lorentz gauge,

$$\underset{\sim}{\nabla} \cdot \hat{\underset{\sim}{A}}(\underset{\sim}{x}) - i \frac{\omega}{c} \hat{\phi}(\underset{\sim}{x}) = 0 \ , \tag{14}$$

into the Maxwell equations, and using (11), the perturbed potentials in Eq. (13) satisfy

$$\nabla_\perp^2 \hat{\underset{\sim}{A}}(\underset{\sim}{x}) = - \frac{4\pi}{c} \hat{\underset{\sim}{J}}(\underset{\sim}{x}) \ , \tag{15}$$

$$\nabla_\perp^2 \hat{\phi}(\underset{\sim}{x}) = - 4\pi\hat{\rho}(\underset{\sim}{x}) \ , \tag{16}$$

where $\hat{\rho}(\underset{\sim}{x})$ and $\hat{\underset{\sim}{J}}(\underset{\sim}{x})$ are the perturbed charge and current densities, which must be determined self-consistently, and the subscript $\perp$ denotes transverse components. The perturbed current density contributed by the background plasma is given by

$$\hat{\underset{\sim}{J}}_p(\underset{\sim}{x}) = \sigma(r)\hat{\underset{\sim}{E}}(\underset{\sim}{x}) = \sigma\left(i\frac{\omega}{c}\hat{\underset{\sim}{A}}(\underset{\sim}{x}) - \underset{\sim}{\nabla}\hat{\phi}(\underset{\sim}{x})\right), \tag{17}$$

where $\sigma(r)$ is the conductivity of the background plasma. Defining an effective potential

$$\hat{\psi}(r) = \hat{A}_z(r) - \hat{\phi}(r)/\beta_b , \tag{18}$$

and using (11), the axial components of Eqs. (15) yield

$$\nabla_\perp^2(\hat{\psi} + \hat{\phi}/\beta_b) + \frac{4\pi\sigma\omega i}{c^2}\left(\hat{\psi} + \frac{\Omega}{\omega\beta_b}\hat{\phi}\right) = -\frac{4\pi}{c}\hat{J}_{bz} , \tag{19}$$

where $\hat{J}_{bz}(\underset{\sim}{x})$ is the axial component of the beam current density.

After some algebraic manipulation of the axial component of Eq. (13a), $\hat{B}_z\hat{\underset{\sim}{e}}_z = \underset{\sim}{\nabla}_\perp \times \hat{\underset{\sim}{A}}_\perp$ , we can show that

$$c\underset{\sim}{\nabla}_\perp \times \hat{B}_z\hat{\underset{\sim}{e}}_z = -ikc\underset{\sim}{\nabla}_\perp\hat{\psi} + i\left(\Omega - \frac{kc}{\beta_b\gamma_b^2}\right)\underset{\sim}{\nabla}_\perp\hat{\phi} + 4\pi\hat{\underset{\sim}{J}}_\perp , \tag{20}$$

where $\hat{\underset{\sim}{J}}_\perp$ is the transverse component of the perturbed current density, $\hat{\underset{\sim}{e}}_z$ is a unit vector in the z-direction, and use has been made of Eqs. (15 - 18). Making use of Eqs. (17) and (20), it is also straightforward to show that for axisymmetric modes (where $B_z$ = const),

$$\frac{1}{r}\frac{\partial}{\partial r}\left(r\frac{\partial}{\partial r}\hat{\phi}\right) = -\frac{1}{r}\frac{\partial}{\partial r}\left\{r\frac{ikc(\partial/\partial r)\hat{\psi} - 4\pi\hat{J}_{br}}{4\pi\sigma - i(\Omega - kc/\beta_b\gamma_b^2)}\right\}$$

$$+\frac{i}{r}\frac{\partial}{\partial r}\left\{r\frac{(4\pi\sigma\omega/c)\hat{A}_r}{4\pi\sigma - i(\Omega - kc/\beta_b\gamma_b^2)}\right\}, \qquad (21)$$

where $\hat{J}_{br}$ and $\hat{A}_r$ are the radial components of the perturbed beam current density and magnetic potential, respectively.

From the continuity equation $-i\omega\hat{\rho} + \nabla \cdot \hat{J} = 0$, and the perturbed Poisson equation, it is evident that the perturbed electric potential $\hat{\phi}(r)$ is at most of order $4\pi R_b^2 \nabla \cdot \hat{J}_b/(4\pi\sigma - i\omega)$. Substituting Eq. (21) into Eq. (19) and using (10) we therefore obtain the eigenvalue equation for axisymmetric modes,

$$\frac{1}{r}\frac{\partial}{\partial r}\left\{r\frac{4\pi\sigma - i\omega}{4\pi\sigma - i(\Omega - kc/\beta_b\gamma_b^2)}\frac{\partial}{\partial r}\hat{\psi}(r)\right\} + \frac{4\pi\sigma\omega i}{c^2}\hat{\psi}(r)$$

$$= -4\pi\left\{\frac{\hat{J}_{bz}(r)}{c} + \frac{1}{\beta_b r}\frac{\partial}{\partial r}\left[\frac{r\hat{J}_{br}(r)}{4\pi\sigma - i(\Omega - kc/\beta_b\gamma_b^2)}\right]\right\}, \qquad (22a)$$

where the perturbed beam current density $\hat{J}_b = \hat{J}_{bz}\hat{e}_z + \hat{J}_{br}\hat{e}_r$ is to be calculated from the Vlasov equation. We find in all cases that $\hat{J}_{bz}$ is the driving term in the regime $4\pi\sigma \gtrsim c$, but that $\hat{J}_{br}$ must be retained in going to the small $\sigma$ limit.

We begin our analysis of the Vlasov equation by using the method of characteristics and neglecting initial perturbations, to write the perturbed beam electron distribution in the form

$$\hat{f}_b(x,p) = \frac{e}{\beta_b c}\int_{-\infty}^{0} d\tilde{z}\, \exp(-i\Omega\tilde{z}/\beta_b c)\{\hat{E}(x') + \frac{1}{c}[v' \times B(x')]\}\cdot\frac{\partial}{\partial p'} f_b^0 ,$$

where $\tilde{z} = z' - z$, and the particle trajectories $\underset{\sim}{x}'(z')$ and $\underset{\sim}{v}'(z')$ satisfy the "initial" condition $\underset{\sim}{x}'(\tilde{z} = 0) = \underset{\sim}{x}$, and $\underset{\sim}{v}'(\tilde{z} = 0) = \underset{\sim}{v}$. Within the context of Eq. (10), the perturbed beam electron distribution in Eq. (11) can be further simplified as[7]

$$\hat{f}_b(r,p) = \frac{e\gamma_b m\beta_b}{p_\perp} \frac{\partial f_b^0}{\partial p_\perp}\left[\hat{\psi}(r) + \frac{\Omega}{v_z}\int_{-\infty}^{0} d\tilde{z} i\hat{\psi}(r')\exp(-i\psi\tilde{z}/v_z)\right]$$

$$+ \frac{\omega e}{v_z c}\frac{\partial f_b^0}{\partial p_z}\int_{-\infty}^{0} d\tilde{z} i\hat{\psi}(r')\exp(-i\psi\tilde{z}/v_z) \ ,$$

where $p_\perp$ is the transverse momentum in a frame of reference rotating at frequency $\omega_b$, i.e., by $p_\perp^2 = p_r^2 + (p_\theta - \gamma_b m\omega_b r)^2$. The perturbed beam current density can then be expressed as a velocity moment of $\hat{f}_b(r,\underset{\sim}{p})$,

$$\hat{\underset{\sim}{J}}_b(r) = -2\pi e^2\beta_b\int_0^{2\pi}\frac{d\phi}{2\pi}\int p_\perp dp_\perp \int dp_z \underset{\sim}{p}\left\{\frac{1}{p_\perp}\frac{\partial f_b^0}{\partial p_\perp}\hat{\psi}(r)\right.$$

$$\left. + \frac{1}{v_z}\left[\frac{\Omega}{p_\perp}\frac{\partial f_b^0}{\partial p_\perp} + \frac{\omega}{\gamma m\beta_b c}\frac{\partial f_b^0}{\partial p_z}\right]\int_{-\infty}^{0} d\tilde{z} i\hat{\psi}(r')\exp(-i\psi\tilde{z}/v_z)\right\} , \qquad (22b)$$

where we have again used (10) and the property that $\hat{A}_r(r)$ is order of $\hat{\psi}(r)$ or less. The integro-differential eigenvalue equation for azimuthally symmetric perturbations, Eqs. (22a,b), constitutes a principal result of this article, and can be used to investigate stability properties quite rigorously for a broad range of system parameters. The source term in Eq. (22b) contains an integral of the unknown eigenfunction $\hat{\psi}(r)$ over the equilibrium particle orbits, which makes the equation rather intractable, in general. However, it is possible to obtain analytic solutions to Eq. (22) for some ranges of physical parameters. In the remainder of this

paper, we investigate the stability properties of the analytic solutions to Eq. (22).

In order to carry out the orbit integration in Eq. (22b), it is useful to introduce Cartesian coordinates (x,y) which are related to the polar coordinates $(r,\theta)$ by $x = r\cos\theta$, $y = r\sin\theta$, and to note that the polar momentum variables $(p_\perp,\phi)$ in the rotating frame are related to $p_x$ and $p_y$ by $p_x + \gamma_b m\omega_b y = p_\perp\cos\phi$, and $p_y - \gamma_b m\omega_b x = p_\perp\sin\phi$, where $p_\perp^2 = p_r^2 + (p_\theta - \gamma_b m\omega_b r)^2$. For the case under consideration, where the unperturbed net current is uniform out to $r = R_b$, the perpendicular electron trajectories can then be expressed as[5]

$$x'(\tilde{z}) = \frac{1}{\omega_b^+ - \omega_b^-}\left\{\frac{p_\perp}{\gamma_b m}\{\sin(\phi + \omega_b^+\tilde{z}/v_z) - \sin(\phi + \omega_b^-\tilde{z}/v_z)\}\right.$$

$$\left. + r(\omega_b - \omega_b^-)\cos(\theta + \omega_b^+\tilde{z}/v_z) - r(\omega_b - \omega_b^+)\cos(\theta + \omega_b^-\tilde{z}/v_z)\right\}, \quad (23a)$$

$$y'(\tilde{z}) = \frac{1}{\omega_b^+ - \omega_b^-}\left\{\frac{p_\perp}{\gamma_b m}\{\cos(\phi + \omega_b^-\tilde{z}/v_z) - \cos(\phi + \omega_b^+\tilde{z}/v_z)\}\right.$$

$$\left. + r(\omega_b - \omega_b^-)\sin(\theta + \omega_b^+\tilde{z}/v_z) - r(\omega_b - \omega_b^+)\sin(\theta + \omega_b^-\tilde{z}/v_z)\right\}, \quad (23b)$$

where the frequencies $\omega_b^\pm$ are defined in Eq. (6). In the next section, we shall develop an approximation scheme for solving the coupled equations (22), based on exact solutions to Eqs. (22) and (23) that can be obtained in the limit $|4\pi\sigma R^2\omega/c^2| \ll 1$.

## IV. DISPERSION RELATIONS FOR THE AXISYMMETRIC MODES

We shall proceed with the stability analysis of the azimuthally symmetric modes for the particular configuration illustrated in Fig. 1, wherein the plasma conductivity profile is specified to be a step function,

$$\sigma(r) = \begin{cases} \hat{\sigma}_1, & 0<r<R_b \ , \\ \hat{\sigma}_2, & R_b<r<R_c \ , \end{cases} \tag{24}$$

with $\hat{\sigma}_2$ so small that

$$\hat{\sigma}_2 R_c^2 << \hat{\sigma}_1 R_b^2 \ . \tag{25}$$

This type of conductivity profile is reasonable for a beam propagating in and ionizing a neutral or weakly pre-ionized gas. The dependence of stability properties on the form of the conductivity profile is of considerable interest, but will not be considered in full generality in the present paper.

The method used to derive approximate dispersion relations is as follows. We define a characteristic magnetic decay time

$$\tau_d = \pi \hat{\sigma}_1 R_b^2 / 2c^2 \ . \tag{26}$$

Each mode has a different characteristic magnetic decay time which differs from (26) by a numerical factor. It is convenient to use (26), which defines the dipole decay time for the hose mode, as a reference

decay time throughout the paper.] In the limit $\omega\tau_m << 1$, solutions of Eqs. (22) can be found, with the form

$$\hat{\psi}_n(r) = \sum_{j=o}^{n} a_j (r/R_b)^{2j} , \quad 0 \le r \le R_b , \tag{27}$$

and the quadrature of Eq. (22b) can be performed analytically to yield expressions for $\hat{J}_{\sim b}$ in terms of $\hat{\psi}$. On the assumption that these expressions for $\hat{\psi}(r)$ are reasonably accurate in the whole range $0 < \omega\tau_m \lesssim 1$, we proceed to use these expressions for $\hat{J}_{\sim b}$ in terms of $\hat{\psi}$ in the full Eq. (22a), including the $\omega\tau_m$ term, thus reducing Eqs. (22) to an ordinary differential equation for $\hat{\psi}$. This equation could be solved exactly for a dispersion relation $\Omega(\omega)$ (in terms of Bessel functions), but in the spirit of the preceding analysis we choose rather to produce a variational approximation to the dispersion relation, using $\hat{\psi}_n$ as the trial eigenfunction. One or more modes are found for each radial mode number n, with n = 1 corresponding to the usual sausage mode and n = 2 to beam hollowing modes.

A. n = 1 Sausage Mode

As a first example, we consider the n = 1 eigenfunction. In the limit of small magnetic decay time,

$$\frac{4}{3}\,\omega\tau_d << 1, \tag{34a}$$

the eigenfunction

$$\hat{\psi}(r) = \begin{cases} a_o(1-r^2/R_b^2) & , \ 0 \le r \le R_b \\ 0 & , \ R_b \le r \le R_c \end{cases} \tag{35}$$

is a self-consistent solution to Eq. (22), as shown in the previous literature.[3] Since we perturb about this solution, the stability analysis in this section is restricted to the regime

$$\frac{4}{3}\,\omega\tau_d \lesssim 1 \ . \tag{34b}$$

The perturbed beam current density can be calculated in closed form by substituting Eq. (35) into Eq. (22b) and using Eq. (23). The result for $\hat{J}_{bz}$, the axial component of the perturbed current density, is

$$\hat{J}_{bz}(r) = \frac{c\beta_b^2}{4\pi}\ \frac{1}{r}\frac{\partial}{\partial r}\left\{ r\ \frac{\omega_{pb}^2(r)}{\Omega^2 - (\omega_b^+ - \omega_b^-)^2}\ \frac{\partial}{\partial r}\ \hat{\psi}(r) \right\}, \tag{36}$$

where the plasma frequency function $\omega_{pb}(r)$ is defined by

$$\omega_{pb}^2(r) = \begin{cases} \hat{\omega}_{pb}^2, & 0 \le r < R_b \ , \\ 0, & R_b < r \le R_c \ , \end{cases} \tag{37}$$

and the fast and slow rotational frequencies $\omega_b^{\pm}$ for beam electrons are defined in Eq. (6). Similarly, the radial component of perturbed current density is found to be

$$\hat{J}_{br}(r) = \frac{i}{4\pi} \frac{\omega_{pb}^2(r)\beta_b\Omega}{\Omega^2 - (\omega_b^+ - \omega_b^-)^2} \frac{\partial}{\partial r}\hat{\psi}(r) \ . \tag{38}$$

Equations (36)-(38) show that this mode consists of a self-similar expansion and contraction of the beam slices, without altering the flat-topped beam profile or mixing beam electrons at different axial coordinates $\tau$ within the beam. This is the usual sausage mode.

Substituting Eq. (36) and (38) into Eqs. (22) and carrying out a simple algebraic manipulation, we obtain the eigenvalue equation,

$$\frac{1}{r}\frac{\partial}{\partial r}\left\{\frac{r(\partial\hat{\psi}/\partial r)}{4\pi\sigma - i(\Omega - kc/\beta_b\gamma_b^2)}\left[4\pi\sigma - i\omega + \frac{\omega_{pb}^2(r)}{\Omega^2 - (\omega_b^+ - \omega_b^-)^2}\left(4\pi\sigma\beta_b^2 + \frac{i\omega}{\gamma_b^2}\right)\right]\right\} + \frac{4\pi\sigma\omega i}{c^2}\hat{\psi}(r) = 0, \tag{39}$$

for the n = 1 perturbation. Equation (35) is clearly a self consistent solution to Eq. (39) in the limit $\omega\tau_d \to 0$ (i.e. the last term can be neglected), provided that $\Omega(\omega)$ satisfies the dispersion relation

$$4\pi\hat{\sigma}_1 - i\omega + \frac{\hat{\omega}_{pb}^2}{\Omega^2 - (\omega_b^+ - \omega_b^-)^2}\left(4\pi\hat{\sigma}_1\beta_b^2 + \frac{i\omega}{\gamma_b^2}\right) = 0 \ ,$$

In order to find an approximate dispersion relation which includes the influence of the magnetic decay time without going through a Bessel function analysis of Eq. (39), we multiply Eq. (39) by $r\hat{\psi}(r)$ and integrate

over r from r = 0 to r = $R_c$. It was shown in Ref. 7 that if a trial function $\hat{\psi}_t$ is substituted in the integrals, this procedure gives a dispersion relation $\Omega(\omega)$ that is accurate to second order in the error in $\hat{\psi}_t$. Thus the procedure can be described as a variational approximation, although it does not give a lower bound, because the differential operator is non-Hermitian. The result is a dispersion relation

$$(4\pi\hat{\sigma}_l - i\omega)\left(1 - \frac{4}{3} i\omega\tau_d\right) + \frac{\hat{\omega}_{pb}^2}{\Omega^2 - (\omega_b^+ - \omega_b^-)^2}\left(4\pi\hat{\sigma}_l\beta_b^2 + i\frac{\omega}{\gamma_b^2}\right) = 0 \qquad (40)$$

where use has been made of Eq. (10). In the limit of a nonneutral electron beam where $4\pi\hat{\sigma}_l/\omega \to 0$, the dispersion relation in Eq. (40) can be simplified to

$$\Omega^2 = (\omega_b^+ - \omega_b^-)^2 + \hat{\omega}_{pb}^2/\gamma_b^2 \qquad (41)$$

which is identical to the result obtained by Uhm and Davidson.[3] The equilibrium constraint, Eq. (7), indicates that the right-hand side of Eq. (41) is always positive. Thus the n = 1 perturbations about a nonneutral electron beam are stable. Analysis of Eq. (40) will be deferred to Sec. V.

B. n = 2 Hollowing Mode

As a second example, we consider the n = 2 eigenfunction,

$$\hat{\psi}(r) = \begin{cases} a_o (1 - 4r^2/R_b^2 + 3r^4/R_b^4), & 0 \le r \le R_b , \\ 0 , & R_b \le r \le R_c , \end{cases} \tag{42}$$

which is found to be a self-consistent solution to (22) in the limit

$$\frac{4}{15}\,\omega\tau_d << 1 . \tag{43}$$

Substituting Eq. (42) into Eq. (22b) and carrying out some tedious algebraic manipulations that make use of Eq. (10), we can show that the radial and axial components of the perturbed n = 2 current density are

$$\hat{J}_{br}(r) = \frac{i}{4\pi} \frac{\omega_{pb}^2(r)\beta_b\Omega}{\Omega^2 - (\omega_b^+ - \omega_b^-)^2} \left\{ \frac{\partial}{\partial r}\hat{\psi}(r) - 72a_0 \frac{(\omega_b^+ - \omega_b)(\omega_b - \omega_b^-)}{\Omega^2 - 4(\omega_b^+ - \omega_b^-)^2} \frac{r}{R_b^2}\left(2 - 3\frac{r^2}{R_b^2}\right) \right\} , \tag{44}$$

and

$$\hat{J}_{bz}(r) = \frac{c\beta_b^2}{4\pi} \frac{1}{r}\frac{\partial}{\partial r}\, r \frac{\omega_{pb}^2(r)}{\Omega^2 - (\omega_b^+ - \omega_b^-)^2} \frac{\partial}{\partial r}\hat{\psi}(r) - \frac{c\beta_b^2}{4\pi} \frac{72a_0(\omega_b^+ - \omega_b)(\omega_b - \omega_b^-)}{[\Omega^2 - (\omega_b^+ - \omega_b^-)^2][\Omega^2 - 4(\omega_b^+ - \omega_b^-)^2]} \left\{ \hat{\omega}_{pb}^2 \frac{\delta(r - R_b)}{R_b} + 4\frac{\omega_{pb}^2(r)}{R_b^2}\left(1 - 3\frac{r^2}{R_b^2}\right) \right\} \tag{45}$$

where $\omega_b$ is the rotational frequency of the electron beam. We note that

$\hat{J}_{bz}(r)$ is of the form $A_o + A_1 r^2$ within the beam, where $A_o$ and $A_1$ are constants. Thus this mode involves non-self-similar axisymmetric distortions (hollowing or peaking on axis) of the beam profile.

As in the previous section, an approximate eigenvalue equation for $\omega\tau_d \neq 0$ can be determined by substituting Eqs. (44) and (45) into Eq. (22). This gives

$$\frac{1}{r}\frac{\partial}{\partial r}\left\{\left(\frac{4\pi\sigma - i\omega}{4\pi\sigma - i(\Omega - kc/\beta_b\gamma_b^2)} + \Gamma_b(r)\right) r \frac{\partial}{\partial r}\hat{\psi}(r)\right\} + \frac{4\pi\sigma\omega i}{c^2}\hat{\psi}(r)$$

$$= 72a_0 \frac{(\omega_b^+ - \omega_b)(\omega_b - \omega_b^-)}{\Omega^2 - 4(\omega_b^+ - \omega_b^-)^2}\frac{1}{r}\frac{\partial}{\partial r}\left[\Gamma_b(r)\frac{r^2}{R_b^2}\left(2 - 3\frac{r^2}{R_b^2}\right)\right], \qquad (46)$$

where the function $\Gamma_b(r)$ is defined by

$$\Gamma_b(r) = \frac{\omega_{pb}^2(r)}{\Omega^2 - (\omega_b^+ - \omega_b^-)^2}\frac{4\pi\sigma\beta_b^2 + i\omega/\gamma_b^2}{4\pi\sigma - i(\Omega - kc/\beta_b\gamma_b^2)}. \qquad (47)$$

As in the previous section, we multiply Eq. (46) by $r\hat{\psi}(r)$ and integrate over r from $r = 0$ to $r = R_c$, to obtain a variational expression for the dispersion relation in terms of the unknown exact $\hat{\psi}(r)$, and then use Eq. (42) as the trial function. This procedure gives

$$(4\pi\sigma_1 - i\omega)\left(1 - \frac{4}{15}i\omega\tau_d\right)$$

$$+ \frac{\hat{\omega}_{pb}^2(4\pi\hat{\sigma}_1\beta_b^2 + i\omega/\gamma_b^2)}{\Omega^2 - (\omega_b^+ - \omega_b^-)^2}\left(1 + \frac{18(\omega_b^+ - \omega_b)(\omega_b - \omega_b^-)}{\Omega^2 - 4(\omega_b^+ - \omega_b^-)^2}\right) = 0, \qquad (48)$$

where use has been made of Eq. (10). The dispersion relation in Eq. (48) can be used to investigate stability properties of the n = 2 perturbations

for a broad range of physical parameters, and detailed investigations of Eq. (48) will be presented in Sec. V.

As a particular case, we consider Eq. (48) in the limit of a nonneutral electron beam characterized by $4\pi\hat{\sigma}_1/\omega \to 0$. In this case, the dispersion relation in Eq. (48) can be expressed as

$$[\Omega^2 - (\omega_b^+ - \omega_b^-)^2][\Omega^2 - 4(\omega_b^+ - \omega_b^-)^2] \tag{49}$$

$$= \frac{\hat{\omega}_{pb}^2}{\gamma_b^2}\{[\Omega^2 - 4(\omega_b^+ - \omega_b^-)^2] + 18(\omega_b^+ - \omega_b)(\omega_b - \omega_b^-)\} \quad ,$$

which is identical to the results obtained by Uhm and Davidson.[3] Equation (49) is a simple quadratic equation for $\Omega^2$, and the necessary and sufficient condition for instability can be expressed as

$$\frac{(\omega_b^+ - \omega_b)(\omega_b - \omega_b^-)}{(\omega_b^+ - \omega_b^-)^2} > \frac{2}{9}\left[\left(\frac{\gamma_b \omega_{cb}}{\omega_{pb}}\right)^2 - 1\right] \quad . \tag{50}$$

Note that when Eq. (50) is satisfied, the perturbations are purely growing, i.e., $\Omega_r = \mathrm{Re}\Omega = 0$, and that the rotational frequency $\omega_b$ can have a large influence on stability behavior. Equation (49) is also similar in form to the result obtained by Gluckstern[16] for transverse instabilities of proton beams in the quadrupole magnetic fields, which are particularly important in the heavy ion fusion experiment.[12,13]

C. n = 0 Axial Bunching Mode

The n = 0 mode, which is of particular interest for unneutralized beams, is quite different in nature from the n ≥ 1 modes. We find that

$$\hat{\psi}(r) = a_0 \begin{cases} 1, & 0 \le r < R_b , \\ \ell n(r/R_c)/\ell n(R_b/R_c), & R_b < r \le R_c \end{cases} \tag{28}$$

is a solution to Eq. (22) in the limit

$$4\omega\tau_d << 1 . \tag{29a}$$

and

$$R_b << R_c . \tag{29b}$$

Substituting Eq. (28) in Eq. (22b) and using (29b) and the identity $p_r = p_\perp \cos(\phi-\theta)$, we obtain the axial component of the perturbed beam current density,

$$\hat{J}_{bz}(r) = \begin{cases} -e^2\hat{n}_b a_0 \omega^2/(\gamma_b^3 mc\Omega^2) , & 0 \le r < R_b , \\ 0 , & R_b < r \le R_c , \end{cases} \tag{30}$$

and the radial component,

$$\hat{J}_{br}(r) = 0 . \tag{31}$$

Clearly, the n = 0 mode involves purely axial flow, leading to bunching. Because a beam becomes axially rigid in the highly relativistic limit, $\hat{J}_{bz}$ is seen to fall off rapidly as $\gamma_b$ increases. The dispersion relation

that determines the eigenfrequency $\omega$ or $\Omega$ is obtained as in the previous sections, by substituting Eqs. (28), (30), and (31) into Eq. (22), multiplying Eq. (22) by $r\hat{\psi}(r)$ and integrating over r from r = 0 to r = $R_c$. This gives the dispersion relation

$$\frac{\omega + 4\pi i\hat{\sigma}_2}{[(kc/\beta_b) - \omega - 4\pi i\hat{\sigma}_2]\ell n(R_c/R_b)} + 4i\omega\tau_d = \frac{2\nu}{\gamma_b^3}\frac{\omega^2}{\Omega^2} \quad , \tag{32}$$

where $\nu$ is Budker's parameter defined in Eq. (1), a result which is valid only if

$$4\omega\tau_d \leq 1 \quad , \tag{29c}$$

and (29b) is also satisfied.

The dispersion relation in Eq. (32) can be used to investigate stability properties of the azimuthally symmetric surface perturbations about an electron beam in a background plasma with arbitrary values of density and plasma conductivity. In particular, for a nonneutral electron beam in an environment where $4\pi\sigma/\omega \to 0$, Eq. (32) simplifies to

$$\Omega^2 = \frac{2\nu}{\gamma_b^3}(k^2c^2 - \omega^2)\ell n(R_c/R_b) \quad , \tag{33}$$

which is identical to the result obtained by Briggs[8] for the space-charge wave mode where $\omega \simeq kc\beta_b$. Note from Eq. (33) that the space-charge wave is a stable mode because $k^2c^2 > \omega^2$ in this mode. We also note the $\gamma_b^{-3}$ dependence of $\Omega^2$, which occurs because this mode (unlike the $n \geq 1$ modes) involves purely axial flow. A detailed investigation of Eq. (32) will be carried out in Sec. V.

## V. STABILITY PROPERTIES OF AZIMUTHALLY SYMMETRIC PERTURBATIONS

We now investigate stability properties predicted by Eqs. (32), (40), and (48) for $\sigma \neq 0$. Depending upon the way in which a stability problem is phrased, either $\omega$ or $\Omega$ may be regarded as the independent variable, and taken to be real; a complete understanding requires an analysis in the complex plane for both $\omega$ and $\Omega$. We shall concentrate here on the solution of the dispersion relations in Eqs. (32), (40), and (48), for given real values of the oscillation frequency $\omega$; then $\Omega_i$ determines the growth of the wave on a particular beam segment as the beam propagates downstream.

A. Stability Analysis in the High Conductivity Regime

To make the theoretical analysis tractable, we assume that the plasma is collisional to the extent that it is characterized by a real, scalar conductivity. Moreover, we consider in this section the case in which the perturbed beam space charge field is completely neutralized by the plasma, which requires a high conductivity plasma,

$$4\pi\sigma << \omega \; . \tag{51}$$

Within the context of Eq. (51), the dispersion relations in Eqs. (32), (40), and (48) can be simplified considerably.

(a) When (51) is satisfied, the dispersion relation in Eq. (32) for n = 0 reduces to

$$\frac{2\nu}{\gamma_b^3}\frac{\omega^2}{\Omega^2} = 4i\omega\tau_d - \frac{1}{\ell n(R_c/R_b)} \; , \tag{52}$$

which clearly indicates instability. If in addition the magnetic decay time is small, $|4\omega\tau_d \ell n(R_c/R_b)| << 1$, Eq. (52) simplifies further to

$$\Omega^2 = -\frac{2\nu}{\gamma_b^3}\omega^2 \ell n(R_c/R_b) \; , \tag{53}$$

which yields a purely growing mode. Note from Eq. (53) that the growth rate $\Omega_i$ is inversely proportional to $\gamma_b^{3/2}$, which indicates that this unstable mode is important only for a mildly relativistic electron beam satisfying $\gamma_b \lesssim 5$; the rapid fall-off of $\Omega_i$ with $\gamma_b$ is due to the purely axial flow that occurs in this mode. It is instructive to compare

Eq. (53) with Eq. (33), in which the terms proportional to $k^2c^2$ and $\omega^2$ are due to the perturbed beam space charge and magnetic fields, respectively. In a nonneutral electron beam, the stabilizing influence of the perturbed space charge field always prevails over the destabilizing influence of the perturbed magnetic field; thus the beam supports only stable space charge waves. However, in a high conductivity plasma characterized by Eq. (51), the stabilizing influence of the perturbed space charge field vanishes; the mode is then unstable, as shown in Eq. (53).

(b) The dispersion relation in Eq. (40) for n = 1 simplifies to

$$\frac{\Omega^2 - (\omega_b^+ - \omega_b^-)^2 + \hat{\omega}_{pb}^2\beta_b^2}{\Omega^2 - (\omega_b^+ - \omega_b^-)^2} = \frac{4}{3} i\omega\tau_d , \qquad (54)$$

when $4\pi\sigma >> \omega$. The instability mechanism can be easily identified in a self-pinched electron beam where the applied magnetic field vanishes and the fractional charge neutralization becomes unity ($\omega_{cb} = 0$, $f_e = 1$). In this particular case, Eq. (54) can be expressed as

$$\frac{\Omega^2 - \hat{\omega}_{pb}^2\beta_b^2(1 - 2 f_m)}{\Omega^2 - 2\hat{\omega}_{pb}^2\beta_b^2(1 - f_m)} = \frac{4}{3} i\omega\tau_d . \qquad (55)$$

Equation (55) clearly indicates that the instability of the n = 1 sausage perturbation is driven by the plasma return current ($f_m$) and the magnetic phase lag ($\omega\tau_d$). Even for a very small magnetic decay time satisfying $\omega\tau_d << 1$, the system supports a purely growing mode whenever the partial current neutralization $f_m$ satisfies

$$f_m > 0.5 \; ; \tag{56}$$

the growth rate of this mode is

$$\Omega_i = \hat{\omega}_{pb}\beta_b(2f_m-1)^{\frac{1}{2}}$$

We note further that Eq. (55) reduces to

$$z^2 = \eta - \beta_b^2\left[1 + i\,\frac{\zeta}{6}\,(\omega R_b/c)^2\right] \; , \tag{57}$$

for the case $\omega\tau_d << 1$. In the limit of $\eta = 2\beta_b^2$, Eq. (57) is remarkably similar to the result obtained by Weinberg[8] within the framework of the coaxial circular electron beam model.

The influence of the magnetic decay time on the stability behavior will be investigated numerically in Sec. VB.

(c) The dispersion relation in Eq. (48) for n = 2 simplifies to

$$\frac{18\hat{\omega}_{pb}^2\beta_b^2\,(\omega_b^+ - \omega_b)(\omega_b - \omega_b^-)}{[\Omega^2-(\omega_b^+ - \omega_b^-)^2][\Omega^2-4(\omega_b^+ - \omega_b^-)^2]} + \frac{\hat{\omega}_{pb}\beta_b^2}{\Omega^2 - (\omega_b^+ - \omega_b^-)^2} \tag{58}$$

$$= -1 + \frac{4}{15}\,i\omega\tau_d \; ,$$

for high conductivity plasmas. We note from Eq. (58) that for n = 2 as well the magnetic phase lag ($\omega\tau_d$) and plasma return current ($f_m$) cause the instability. In order to illustrate the influence of the plasma return current on the stability behavior, we consider Eq. (58) for a self-pinched beam ($\omega_{cb} = 0$, $f_e = 1$) and for a small magnetic decay time

($\omega T_d << 1$). In this particular case, the dispersion relation in Eq. (58) can be further simplified as

$$z^4 - [10(1 - f_m) - 1]z^2 + [16(1 - f_m) + 1](1 - f_m) = 0 , \qquad (59)$$

where the normalized eigenfrequency Z is defined by $Z = \Omega/\hat{\omega}_{pb}\beta_b$, and we have also set $\omega_b = 0$, i.e. we consider the case of a non-rotating pinched beam. Equation (59) is a simple quadratic equation for $Z^2$, and the necessary and sufficient condition for instability can be expressed as

$$f_m > (2 - 3^{1/2}/2)/3 = 0.38 . \qquad (60)$$

In contrast to the case of n = 1, we note from Eq. (59) that the n = 2 perturbations are not always purely growing when Eq. (60) is satisfied, i.e., $Z_r \neq 0$. Unstable n = 2 perturbations can reduce the beam density at axis, leading to a hollow beam profile. Detailed numerical investigations of Eq. (58) are carried out in the next section.

B. Numerical Analysis for Stability Properties

In this section, we summarize the results of numerical studies of the dispersion relations in Eqs. (32), (40), and (48) for a broad range of the beam electron energy $\gamma_b$, the normalized oscillation frequency $\omega R_b/c$, the plasma conductivity parameter

$$\zeta = 4\pi\hat{\sigma}_1/\omega \quad , \tag{61}$$

and the focussing parameter

$$\eta = (\omega_b^+ - \omega_b^-)^2/\hat{\omega}_{pb}^2 \quad . \tag{62a}$$

The analysis in this section is restricted to a self-pinched electron beam with $\omega_{cb} = 0$. [The stabilizing influence of the applied magnetic field ($\omega_{cb}$) on a related instability (resistive hose) is discussed in Ref. 7.] Making use of Eq. (6), we can simplify the parameter $\eta$ in Eq. (61) to

$$\eta = 2[\beta_b^2(1 - f_m) - (1 - f_e)] \quad , \tag{62b}$$

for self-pinched beams. We note that the value of the parameter $\eta$ is limited to the range $0 \le \eta \le 2\beta_b^2$.

Defining the normalized eigenfrequency

$$z = \Omega/\hat{\omega}_{pb} \quad , \tag{63}$$

the dispersion relations in Eqs. (32), (40), and (48) can be expressed as

$$z^2 + \frac{\ell n(R_c/R_b)}{2\gamma_b^2\beta_b^2}\left(\frac{\omega R_b}{c}\right)^2 \frac{(\hat{\sigma}_2/\hat{\sigma}_1)\zeta\beta_b^2 + i/\gamma_b^2}{[(\hat{\sigma}_2/\hat{\sigma}_1)\zeta - i][1 - \frac{i}{2}\zeta(\omega R_b/c)^2\ell n(R_c/R_b)]} = 0, \tag{64}$$

for the n = 0 perturbation,

$$z^2 - \eta + \frac{\zeta\beta_b^2 + i/\gamma_b^2}{(\zeta - i)[1 - i\zeta(\omega R_b/c)^2/6]} = 0 \qquad (65)$$

for the n = 1 perturbation, and

$$(z^2 - \eta)(z^2 - 4\eta) + (z^2 + \frac{1}{2}\eta)\frac{\zeta\beta_b^2 + i/\gamma_b^2}{(\zeta - i)[1 - i\zeta(\omega R_b/c)^2/30]} = 0 \ , \qquad (66)$$

for the n = 2 perturbation. In obtaining Eq. (64), use has been made of Eq. (10). Moreover, we have assumed $\omega_b = 0$ in Eq. (66), which is consistent for self-pinched beams. Equations (64), (65), and (66) clearly show that only the n = 0 mode is influenced by the location of the conducting wall.

Typical numerical results of Eqs. (64) - (66) are summarized in Fig. 2 for $\gamma_b = 1.5$, $(\omega R_b/c)^2 = 0.01$ and the parameter $\eta = 1.11$. Note from Eq. (62) that $\eta = 1.11$ is the largest possible value of $\eta$ for $\gamma_b = 1.5$, corresponding to a space charge neutralized electron beam ($f_e = 1$) with no plasma return current ($f_m = 0$). We note the following features of Fig. 2: (i) The n = 0 and n = 1 unstable modes have $Z_r < 0$, i.e. propagate backward in the beam, while one of the two n = 2 unstable modes [denoted n = 2(+)] has $Z_r > 0$ and the other [n = 2(-)] has $Z_r < 0$. The n = 2(-) mode is always the faster growing of the two. (ii) Each mode, except n = 0, has two maxima of the growth rate $\Omega_i$, the first occurring for all modes at $\zeta \approx 1$, the transition point from electrostatically to magnetically dominated forces, and the second occurring at

$$\zeta \approx 6(c/\omega R_b)^2, \text{ i.e. } \omega\tau_d \approx 3/4, \ (n = 1), \qquad (67a)$$

$$\zeta \approx 30(c/\omega R_b)^2, \text{ i.e. } \omega\tau_d \approx 15/4 \qquad (n = 2). \tag{67b}$$

Note that when $f_m << 1$, the second instability peak is driven by the phase lag $\tau_d$ between the beam oscillations and the magnetic restoring force, and it is appropriate to scale $\omega$ to $\tau_d$. (iii) The n = 1 perturbation is the most unstable azimuthally symmetric mode. (iv) For a space-charge neutralized beam ($f_e = 1$) with $f_m << 1$, the absolute value of Doppler-shifted real frequency can be approximated by $|Z_r| \simeq \eta^{1/2}$ for n = 1, and $|Z_r| \simeq \eta^{1/2}$ and $|Z_r| \simeq 2\eta^{1/2}$ for n = 2 over the entire unstable range of the conductivity parameter $\zeta$ [Fig. 2(b)]. Since this dependence is so simple, $Z_r$ will not be shown in the subsequent figures.

Figure 3 is similar to Fig. 2a, except that a higher frequency ($\omega^2 R_b^2/c^2 = 0.1$) is considered. We note that Eqs. (67) for the location of the magnetic-dominated instability peak are well satisfied; the location of the peak thus moves to the left on a $\zeta$ scale. The first instability peak remains at $\zeta \approx 1$. The growth rate of the n = 0 mode is seen to increase significantly with $(\omega R_b/c)$, but the n = 1 and n = 2 modes depend weakly on this parameter.

In Fig. 4 we consider a highly relativistic ($\gamma_b = 10$) case, again with $f_e = 1$, $f_m = 0$ (which gives $\eta = 1.98$ in this case). The n = 0 mode is not shown since its growth rate is very small for large $\gamma_b$. The most striking change from Figs. 2 and 3 is that the two peak growth rates of each mode have become equal, and in fact the $Z(\zeta)$ curves are symmetric (on a logarithmic scale) about a point $\zeta \sim (\omega R_b/c)^2$. This feature is easily seen to be a consequence of Eqs. (64) - (66). When $\gamma_b >> 1$, each of these equations takes the form

$$F(Z) = \frac{\text{const}}{(1 - A_1/\zeta)(1 - A_2/\zeta)} , \qquad (68)$$

where $F(Z)$ is a function of $Z$ that is different for each of the two modes, and $A_1$ and $A_2$ are constants which take different values for each of the two modes. It follows that $Z(\zeta)$ takes the same value at two points $\zeta_1$ and $\zeta_2 = (A_1/A_2\zeta_1)$, i.e. the $Z(\zeta)$ curve is symmetric (on a log plot) about $\zeta = (A_1/A_2)^{1/2}$.

The dependence of stability properties on the parameter $\eta$ is illustrated in Fig. 5(a) for $\gamma_b = 1.5$, $n = 1$, in Fig. 5(b) for $\gamma_b = 1.5$, $n = 2$, and in Fig. 5(c) for $\gamma_b = 10$, $n = 1$, where the normalized growth rate $Z_i$ is plotted versus $\zeta$ for $(\omega R_b/c)^2 = 0.1$ and several values of the parameter $\eta$. It is evident that as the parameter $\eta$ [defined in Eq. (62)] decreases to zero (e.g. weakly pinched beam--nearly complete current and space charge neutralization), the growth rate increases rapidly, and the strong growth occurs over a broad range of $\omega$, rather than being confined to two sharp peaks. As discussed in Sec. V.A for the high conductivity regime, this remarkable behavior is due to repulsion of the beam current by the plasma return current ($f_m > 0$) flowing in the highly conducting plasma channel. We also note from Fig. 5(b) that the $n = 2$ (+) perturbation is stable for $\eta = 0$: the dispersion relation, Eq. (66), reduces to

$$Z^2 \left( Z^2 + \frac{\zeta\beta_b^2 + i/\gamma_b^2}{(\zeta - i)[1 - i\zeta(\omega R_b/c)^2/30]} \right) = 0 ,$$

which gives only one unstable mode, $n = 2$ (-).

## VI. HOSE INSTABILITY

Although this paper has been concerned primarily with the axisymmetric ($m = 0$) instabilities, essentially the same analysis can be used to treat higher m modes over the full range of values of the background conductivity $\sigma$, provided that $\sigma(r,\tau)$ is r-independent over the range $0 < r < R_c$. In particular, it is of interest to compare the growth characteristics of the $m = 1$ hose instability to those of the axisymmetric modes we have studied. Our analysis of the hose instability will be based on the same equilibrium (Sec. II) except that we now take $\sigma$ to be a constant, which can have any value, over the full range of r and z. We need not make the long wavelength assumption (10); the weaker assumptions (11) and (12) suffice.

For the hose mode, all perturbed quantities are taken to vary as

$$\begin{aligned} \underset{\sim}{\Phi}(\underset{\sim}{x},t) &= \hat{\phi}(r)\ \exp\ i(kz + \theta - \omega t) \\ &= \hat{\phi}(r)\ \exp\left[-i(\omega\tau + \Omega z/v_z - \theta)\right] , \end{aligned} \tag{69}$$

so that

$$\nabla_\perp^2 = \frac{1}{r}\frac{\partial}{\partial r}\, r\, \frac{\partial}{\partial r} - \frac{1}{r^2} = \frac{\partial}{\partial r}\frac{1}{r}\frac{\partial}{\partial r}\, r\ .$$

The analysis of Maxwell's equations follows that of Sec. II through Eq. (19), at which point the constancy of $\sigma$ is used in (18) and (19) to show that

$$\begin{aligned} \frac{d}{dr}\frac{1}{r}\frac{d}{dr}\, r\, \hat{\Psi} + \frac{4\pi\sigma\omega\, i}{c^2}\hat{\Psi} = -\frac{4\pi}{(4\pi\sigma - i\omega)\, c}\Bigg\{ 4\pi\sigma - i\left(\Omega - \frac{kc}{\beta_b\gamma_b^2}\right)\hat{J}_{bz} \\ + \frac{c}{r\beta_b}\left[\frac{d}{dr}(r\,\hat{J}_{br}) + i\,\hat{J}_{b\theta}\right]\Bigg\}\ . \end{aligned} \tag{70a}$$

The analysis of the Vlasov equation is similar to that of Sec. II, leading in this case to the expression

$$\hat{\underset{\sim}{J}}_b(r) = -2\pi e^2 \beta_b \int_0^{2\pi} \frac{d\phi}{2\pi} \int dp_\perp \, p \, \frac{\partial f_b^o}{\partial p_\perp} \left\{ \hat{\psi}(r) + (\Omega - \omega_b) \int_{-\infty}^{o} d\tilde{z} \; i\hat{\psi}(r') \exp\left[ i(\theta' - \theta - \Omega\tilde{z}) \right] \right\} \tag{70b}$$

Equations (70) define the m = 1 eigenvalue problem as Eqs. (22) did for m = 0.

In the case of the hose mode, in the limit

$$| \omega \tau_d | \equiv \left| \frac{\pi \sigma \omega R_b^2}{2c^2} \right| < 1 \tag{71}$$

Eqs. (70) support a solution

$$\hat{\psi}(r) = \begin{cases} a_o r \;, & 0 \le r \le R_b \;, \\ a_o R_b^2 (R_c^2 - R_b^2)^{-1} (R_c^2 r^{-1} - r), & R_b \le r \le R_r \end{cases} \tag{72}$$

essentially a distortion free snake like displacement of the beam and the associated electromagnetic fields (within the constraints imposed by the conducting boundary conditions at $r = R_c$). Using the orbit equations (23), Eq. (70b) can then be solved for the perturbed current, with the results

$$\hat{J}_{bz}(r) = -\frac{c}{4\pi} \frac{\hat{\omega}_{pb}^2 \beta_b^2}{(\Omega - \omega_b^-)(\Omega - \omega_b^+)} \frac{\psi(r)}{r} \delta(r - R_b), \tag{73a}$$

$$\hat{J}_{br}(r) = \frac{i\beta_b (\Omega - \omega_b)}{4\pi} \frac{\psi(r)}{r} \frac{\omega_{pb}^2(r)}{(\Omega - \omega_b^-)(\Omega - \omega_b^+)}, \tag{73b}$$

$$\hat{J}_{b\theta}(r) = i\, J_{br}(r) + \frac{\omega_3 r}{\beta_b c}\, J_{bz}(r). \tag{73c}$$

For finite values of $\omega\tau_d$, we follow the same approximation scheme used in Sec. IV to derive the dispersion relation. Equation (73) is used in Eq. (70a) to derive the dispersion relation,

$$\frac{1}{2}\frac{d}{dr}\left\{\frac{1}{r}\left[4\pi\sigma - i\omega + i(\Omega-\omega_b)\,\frac{\omega_{pb}^2(r)}{(\Omega-\omega_b^-)(\Omega-\omega_b^+)}\right]\frac{d}{dr}(r\hat{\psi})\right\}$$

$$+ \frac{4\pi\sigma\omega i}{c^2}(4\pi\sigma - i\omega)\,\hat{\psi} \tag{74}$$

$$= \left[4\pi\sigma - i\left(\Omega - \frac{kc}{\beta_b\gamma_b^2} - \frac{\omega_b}{\beta_b^2}\right)\right]\frac{\hat{\omega}_{pb}^2\beta_b^2\delta(r-R_b)}{(\Omega-\omega_b^-)(\Omega-\omega_b^+)}\,\frac{\hat{\psi}(r)}{r}.$$

We note that in the high conductivity limit $4\pi\sigma >> |\omega|$, Eq. (74) reduces to the eigenvalue equation previously obtained by the authors,[7]

$$\frac{d}{dr}\frac{1}{r}\frac{d}{dr}\,r\,\hat{\psi} + \frac{4\pi\sigma\omega i}{c^2}\hat{\psi} = \frac{\hat{\omega}_{pb}^2\beta_b^2}{(\Omega-\omega_b^-)(\Omega-\omega_b^+)}\,\frac{\hat{\psi}}{r}\,\delta(r-R_b). \tag{75}$$

As in Sec. IV, we proceed by multiplying both sides of Eq. (74) by $r\,\hat{\psi}$ and integrating over r from r = 0 to r = $R_c$, thereby obtaining a variational expression for the dispersion relation $\Omega(\omega)$,

$$-\int_0^{R_c}\frac{dr}{r}\left(4\pi\sigma - i\omega + \frac{i(\Omega-\omega_b)\omega_{pb}^2(r)}{2(\Omega-\omega_b^+)(\Omega-\omega_b^-)}\right)\left[\frac{d}{dr}(r\hat{\psi})\right]^2$$

$$+ \frac{-4\pi i\sigma\omega}{c^2}(4\pi\sigma - i\omega)\int_0^{R_c} dr\, r\,\hat{\psi}^2 \tag{76}$$

$$= \left[4\pi\sigma - i\left(\Omega - \frac{kc}{\beta_b\gamma_b^2} - \frac{\omega_{pb}}{\beta_b^2}\right)\right]\frac{\hat{\omega}_{pb}^2\beta_b^2\left[\hat{\psi}(R_b)\right]^2}{(\Omega-\omega_b^+)(\Omega-\omega_b^-)}.$$

We then use Eq. (72) as the trial function $\hat{\psi}(r)$ in (72), finally arriving at an approximate dispersion relation

$$4\pi\sigma \left( 2g_f + \frac{\hat{\omega}_{pb}^2 \beta_b^2}{(\Omega-\omega_b^+)(\Omega-\omega_b^-)} \right) + i\omega \left( -2g_f + \frac{\hat{\omega}_{pb}^2 \gamma_b^{-2}}{(\Omega-\omega_b^+)(\Omega-\omega_b^-)} \right) \tag{77}$$

$$= \frac{4\pi i\sigma\omega}{c^2} (4\pi\sigma - i\omega) g_f R_b^2 \left[ g_f \ln (R_c/R_b) - \frac{1}{2} \right] ,$$

where

$$g_f \equiv (1 - R_b^2/R_c^2)^{-1} .$$

Equation (77) can be used to investigate hose stability properties over a broad range of system parameters, including conductivity $\sigma$, fractional charge and current neutralization $f_e$ and $f_m$, applied magnetic field strength ($\omega_{cb}$), electron energy ($\gamma_b$), and proximity to the conducting guide ($R_b/R_c$). In the limit of $4\pi\sigma << |\omega|$ of low background conductivity, Eq. (77) reduces to the result obtained by Uhm and Davidson,[5]

$$g_f = \frac{\hat{\omega}_{pb}^2}{2\gamma_b^2 (\Omega-\omega_b^-)(\Omega-\omega_b^+)} , \tag{78}$$

which leads only to stable oscillations. On the other hand, in the high conductivity regime $4\pi\sigma >> |\omega|$, Eq. (77) reduces to our previous result,[7]

$$2g_f + \frac{\hat{\omega}_{pb}^2 \beta_b^2}{(\Omega-\omega_b^-)(\Omega-\omega_b^+)} = \frac{4\pi\sigma\omega i}{c^2} g_f R_b^2 \left[ g_f \ln \frac{R_c}{R_b} - \frac{1}{2} \right] . \tag{79}$$

For comparison with the results of Sec. V for the axisymmetric instabilities, we present a number of numerical solutions of Eq. (77) for Re $\Omega(\omega)$ and Im $\Omega(\omega)$, specifying $\omega_b = \omega_{cb} = 0$ and $R_b/R_c = 0.5$, but surveying a broad range of beam electron energy $\gamma_b$, normalized frequency $\omega R_b/c$, normalized conductivity $\zeta$, and focussing parameter $\eta$. These results have been plotted as the dashed curves in Figs. 2-4, along with the results for the various axisymmetric modes (solid curves). The hose dispersion relation is seen to be remarkably similar to those of the axisymmetric modes. In Figs. 2-4 (cases with no return current), the hose growth rate $\Omega_i$ is seen to have two sharp peaks, the first at $\zeta \approx 1$ and the second at

$$\zeta \approx 3(c/\omega R_b)^2, \quad \text{i.e. } \omega\tau_d \approx 0.4 . \tag{80}$$

Both the location of the peak growth rate given by Eq. (80) and the value of the peak growth rate depend to some extent on the value of $R_b/R_c$; the corresponding results for the axisymmetric modes are independent of $R_c$. The peak hose growth rates plotted in Figs. 2-4 for $R_b/R_c = \frac{1}{2}$ lie between those of the $n = 0$ and $n = 1$ axisymmetric modes; for $R_b/R_c \to 0$, however, the hose growth rates would be slightly greater than those of the axisymmetric modes. In the limit of large $\gamma_b$, Eq. (77) can be put in the form (68), so that the two-peaked structure of $Z(\zeta)$ becomes symmetric on a log $\zeta$ plot, as seen in Fig. 4 for all modes. As the return current increases, i.e. $\eta$ decreases to zero, the growth spectrum of the hose mode broadens and becomes singly peaked, and the maximum growth rate increases significantly. Like the sausage and hollowing modes, the hose is driven strongly unstable by the mutual repulsion between the beam current and return current, when the latter has the same equilibrium radial profile as the former.

## VII. CONCLUSIONS

In this paper, we have investigated the stability properties of both azimuthally symmetric ($\partial/\partial\theta = 0$, or $m = 0$) and hose ($m = 1$)) perturbations in an intense particle beam propagating parallel to a uniform applied magnetic field $B_0\hat{e}_z$ through a background plasma. The analysis was carried out within the framework of the Vlasov-Maxwell equations, assuming long wavelength, low frequency perturbations. The analysis was simplified by considering only step-function, time-independent conductivity profiles, by requiring that the plasma charge and current density have the same radial profile as the beam, and by considering a beam with a "loss cone" distribution function, in which all of the beam electrons have the same value of axial canonical momentum and the same value of energy in a frame of reference rotating with angular velocity $\omega_b$. This distribution leads to a flat-topped beam radial profile; the unperturbed beam electron orbits are then simply harmonic at a single frequency.

Equilibrium properties were calculated in Sec. II. The formal stability analysis for azimuthally symmetric perturbations was carried out in Sec. III and an integro-differential eigenvalue equation was obtained, which included beam electron thermal effects and applied generally to any radial mode number. In Sec. IV, dispersion relations for the axisymmetric modes with radial mode numbers $n = 0$, 1, and 2 were obtained analytically from the integro-differential eigenvalue equation (22), for a moderate value of the magnetic decay time such that $\omega T_d \lesssim 1$. Also discussed in Sec. IV were the stability properties of a nonneutral electron beam characterized by $4\pi\hat{\sigma}_1/\omega = 0$. A parallel treatment of the hose mode was carried through in Sec. VI.

Analytic and numerical investigations of the n = 0, 1, and 2 axisymmetric dispersion relations were carried out in Sec. V, and the hose dispersion relation in Sec. VI, for a collision-dominated background plasma. It was shown that the n = 1 and n = 2 axisymmetric modes and the hose mode are all driven unstable by both the plasma return current ($f_m$) and the magnetic decay time ($\omega T_d$). Even for a very small magnetic decay time, the system can be unstable whenever the fractional current neutralization satisfies $f_m > 0.5$ for n = 1 and $f_m > 0.38$ for n = 2. We found that the n = 1 perturbation is the most unstable axisymmetric mode, with maximum growth rate $Z_i = 0.205$, for a relativistic beam with $f_m = 0$, slightly less than that of the resistive hose instability when $R_b/R_c = 0$, but greater than the hose growth rate when $R_b/R_c \geq \frac{1}{2}$. Finally, it has been found in the case of zero plasma return current ($f_m = 0$) that the growth rate of instability has two local maxima corresponding to the electrostatic regime ($4\pi\hat{\sigma}_1 = \omega$) and to the regime where the instability is driven by the magnetic decay time ($\omega T_d \sim 1$).

The resistive hose instability, in the high conductivity regime, has been studied[6,7] for rounded beam profiles which introduce dispersive anharmonic effects. It is of considerable interest to extend the analysis of the axisymmetric modes in this way, as well as to study the effects of more general conductivity and plasma current geometries. It is believed that the hose and axisymmetric modes respond differently to these generalizations of the equilibrium. Such effects will be considered in future work.

## ACKNOWLEDGMENTS

This research was supported in part by the Independent Research Fund at the Naval Surface Weapons Center and in part by Defense Advanced Research Projects Agency (DOD) under ARPA Order No. 3718, Amendment No. 12.

## REFERENCES


1. R. C. Davidson and H. S. Uhm, Phys. Fluids 22, 1375 (1979).
2. D. A. Hammer and N. Rostoker, Phys. Fluids 13, 183 (1970).
3. H. S. Uhm and R. C. Davidson, Phys. Fluids 23, 1586 (1980).
4. M. N. Rosenbluth, Phys. Fluids 3, 932 (1960).
5. H. S. Uhm and R. C. Davidson, Phys. Fluids 23, 813 (1980).
6. E. P. Lee, Phys. Fluids 21, 1327 (1978).
7. H. S. Uhm and M. Lampe, Phys. Fluids 23, 1574 (1980).
8. S. Weinberg, J. Math. Phys. 8, 614 (1967).
9. J. S. DeGassie and J. H. Malmberg, Phys. Rev. Lett. 39, 1078 (1977).
10. J. H. Malmberg and T. M. O'Neil, Phys. Rev. Lett. 39, 1334 (1977).
11. M. Reiser, W. Namkung, and M. A. Brennan, IEEE Trans. Nucl. Sci. NS-26, 3026 (1979).
12. T. Haber and A. W. Maschke, Phys. Rev. Lett. 42, 1479 (1979).
13. S. Abbott, W. Chupp, A. Faltens, W. Herrmannsfeldt, E. Hoyer, D. Keefe, C. H. Kim, S. Rosenblum, and J. Shiloh, IEEE Trans. Nucl. Sci. NS-26, 3095 (1979).
14. C. A. Kapetanakos, Appl. Phys. Lett. 25, 481 (1974).
15. E. J. Lauer, R. J. Briggs, T. J. Fessendon, R. E. Hester, and E. P. Lee, Phys. Fluids 21, 1344 (1978).
16. R. L. Gluckstern, Proc. 1970 Proton Linac Conf. edited by M. R. Tracy, (National Accel. Lab., Batavia, Ill., 1970) p. 811.
17. E. P. Lee, S. Yu, H. L. Buchanan, F. W. Chambers, M. N. Rosenbluth, UCRL-83298, Lawrence Livermore Laboratory (1979).
18. R. J. Briggs, Phys. Fluids 19, 1257 (1976).
19. E. P. Lee, Lawrence Livermore Laboratory Report UCID-16734 (1975).

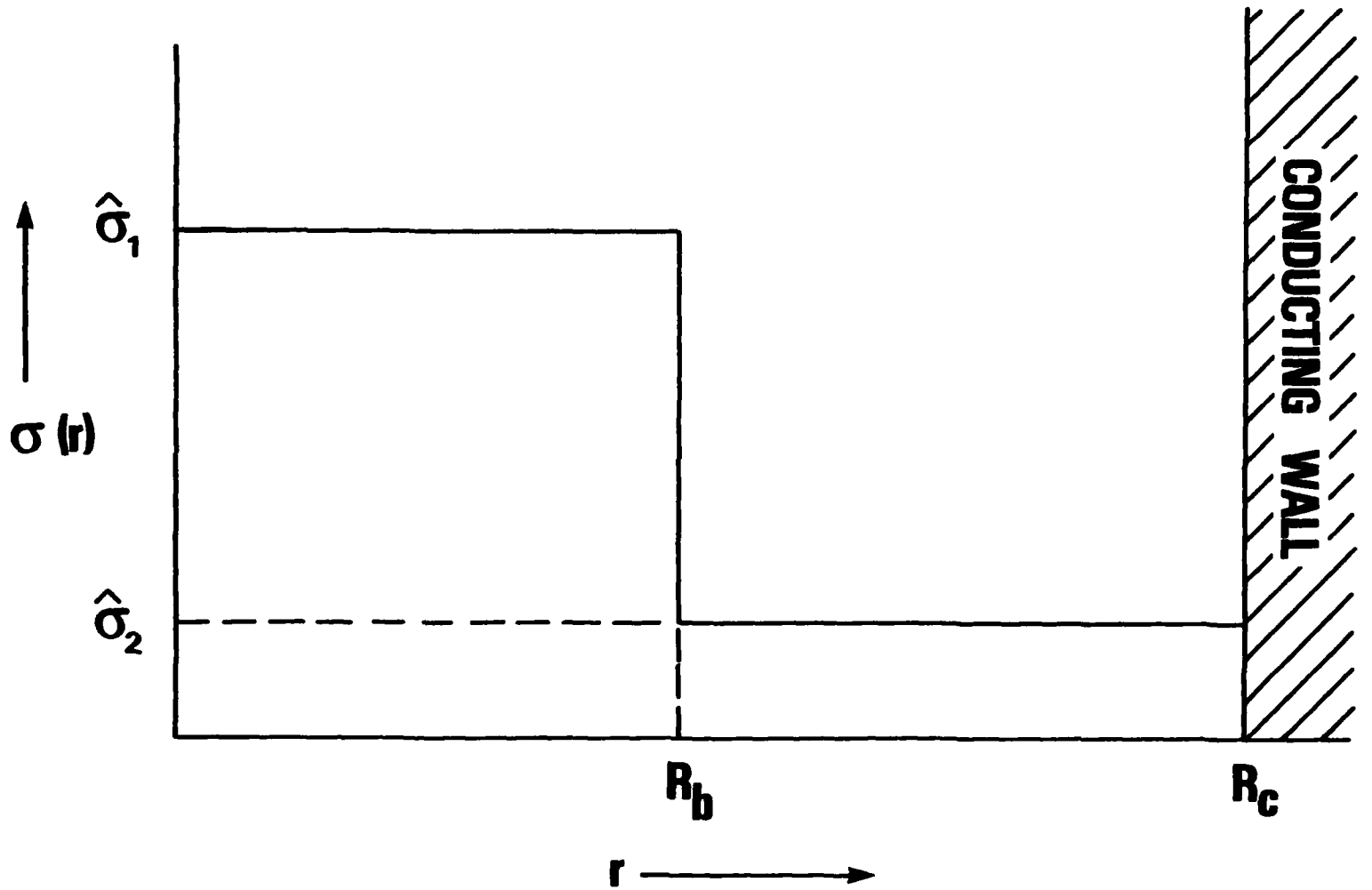


Fig. 1 - Plasma conductivity profile [Eq. (24)].

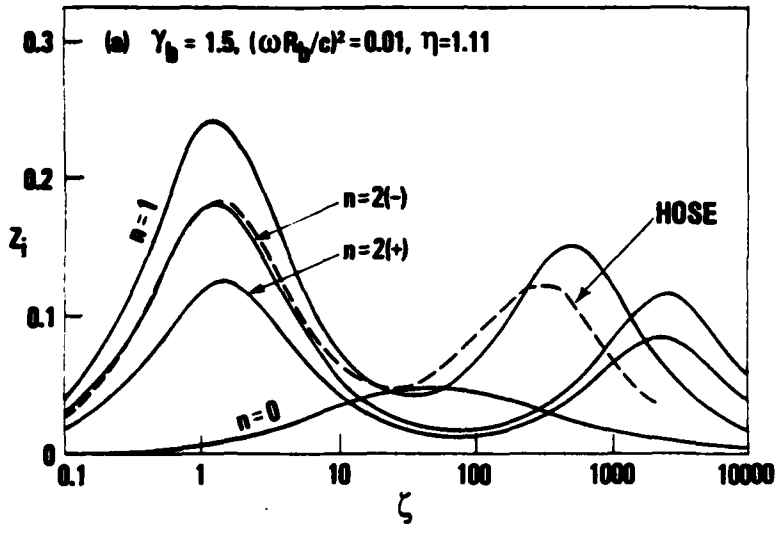


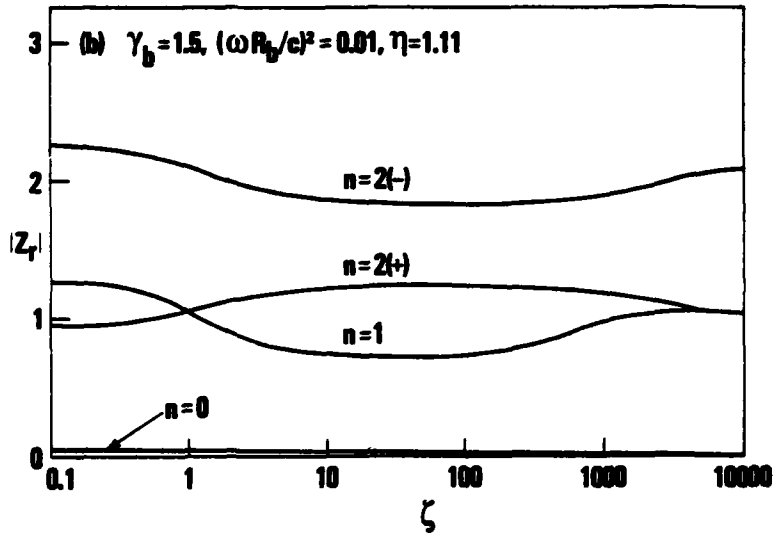


Fig. 2 - Plots of normalized (a) growth rate and (b) Doppler-shifted real frequency versus $\zeta$ [Eqs. (64) - (66)] for $\gamma_b = 1.5$, $(\omega R_b/c)^2 = 0.01$, $\eta = 1.11$ and several values of radial mode number.

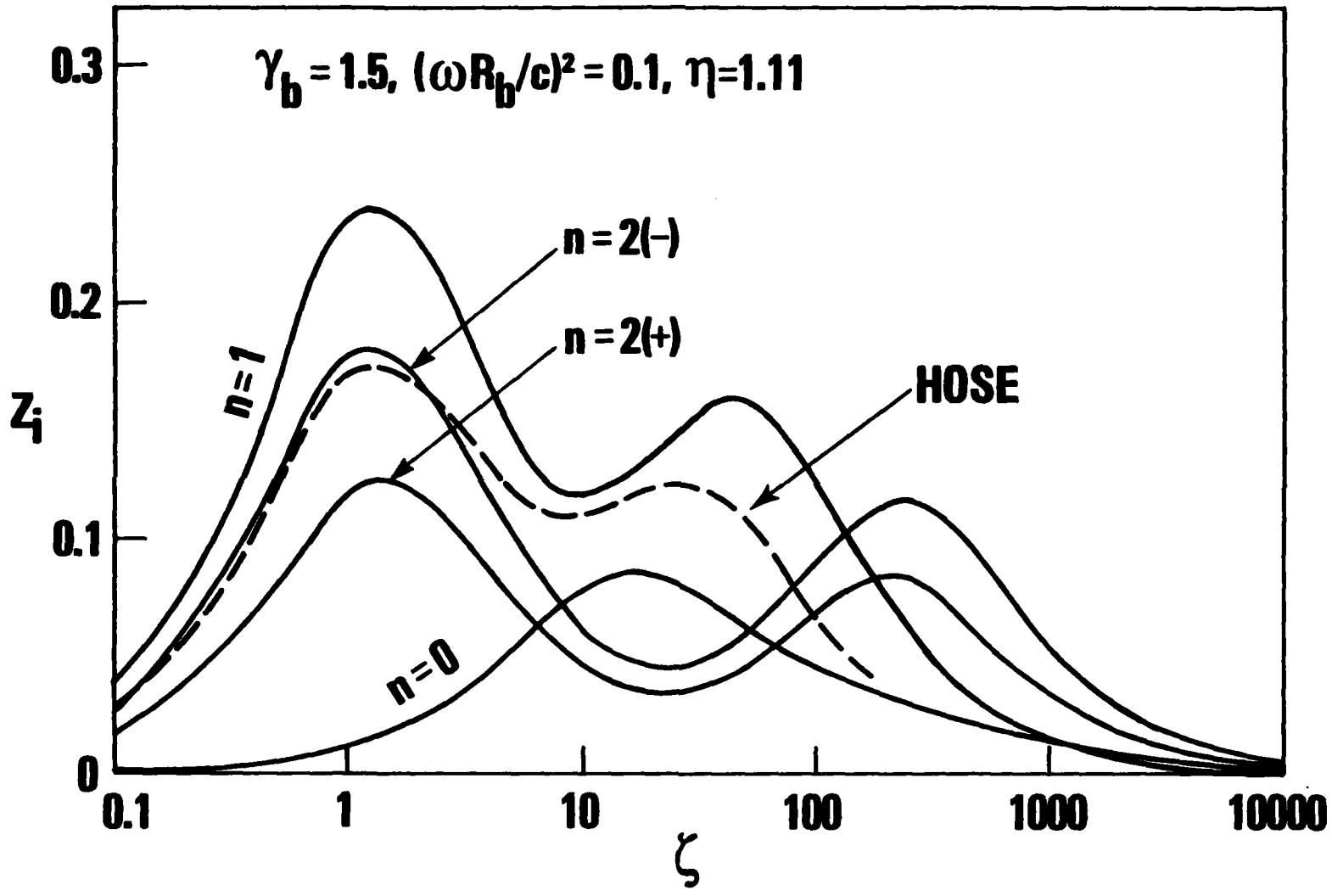


Fig. 3 - Plots of normalized growth rate $Z_i$ versus $\zeta$ [Eqs. (64) - (66)] for $(\omega R_b/c)^2 = 0.1$ and parameters otherwise identical to Fig. 2.

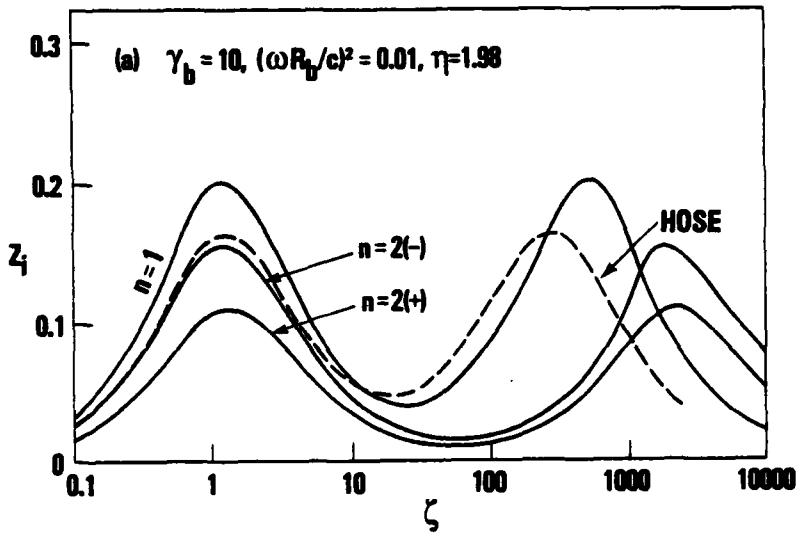


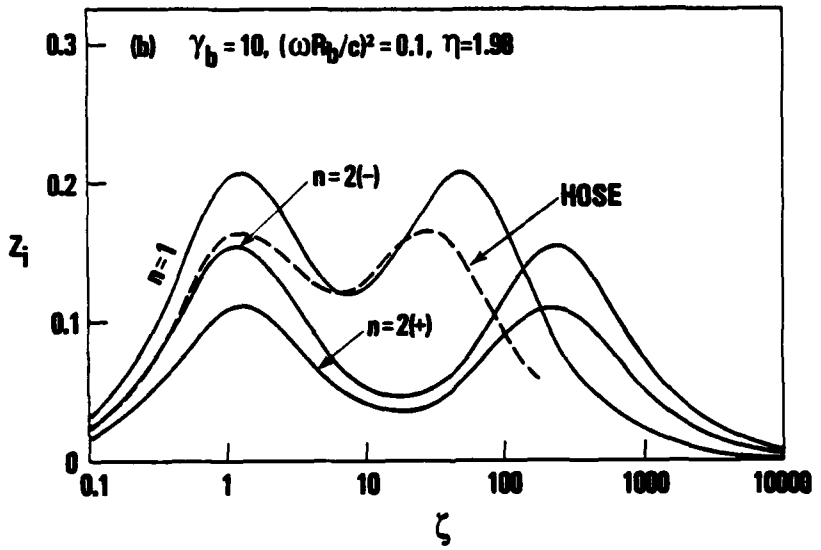


Fig. 4 - Plots of normalized growth rate $Z_i$ versus $\zeta$ [Eqs. (65) and (66)] for $\gamma_b = 10$, (a) $(\omega R_b/c)^2 = 0.01$, (b) $(\omega R_b/c)^2 = 0.1$, and parameters otherwise identical to Fig. 2.

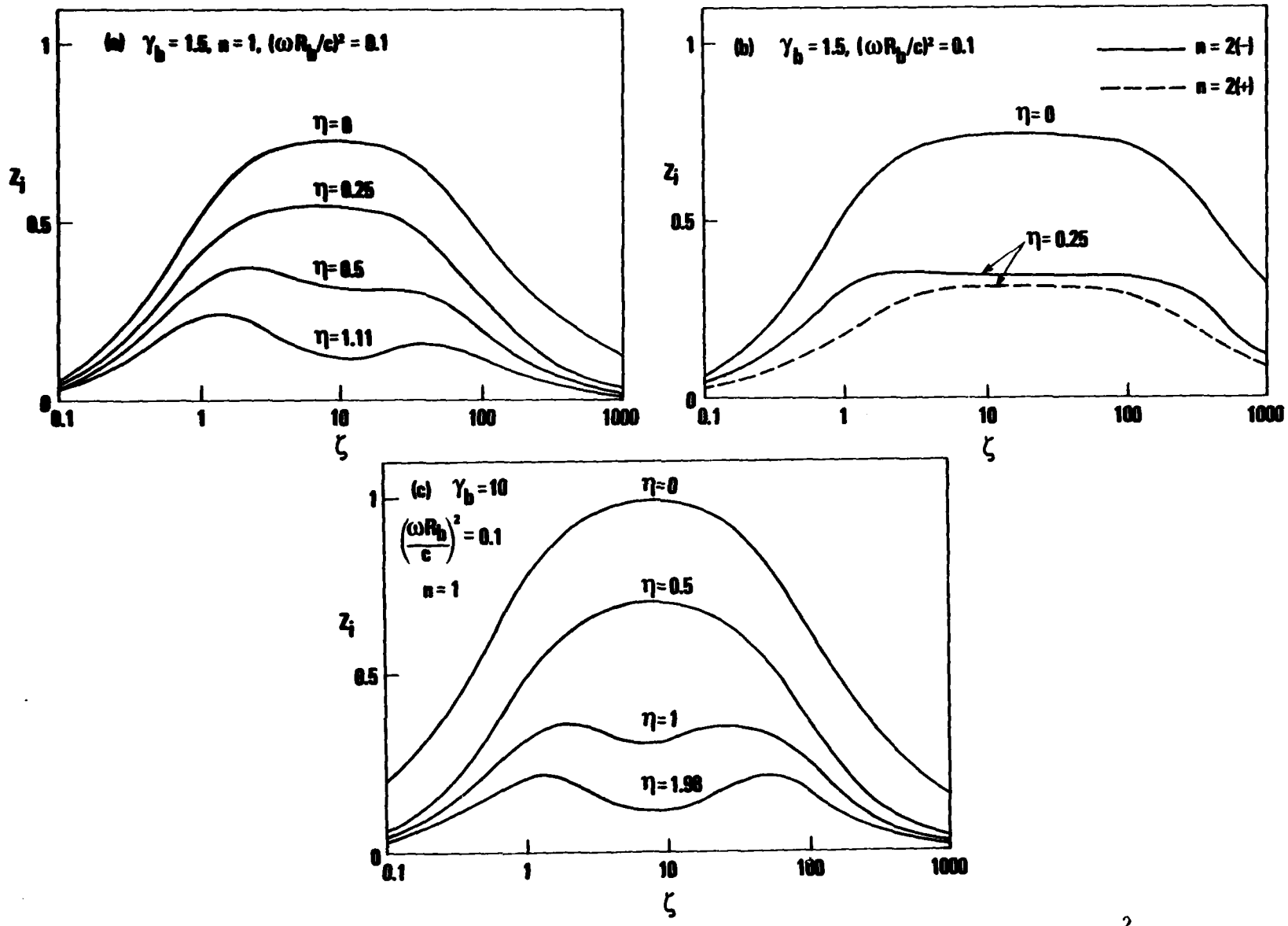


Fig. 5 - Plots of normalized growth rate $Z_i$ versus $\zeta$ [Eqs. (65) and (66)] for $(\omega R_b/c)^2 = 0.1$, (a) $\gamma_b = 1.5$, n = 1, (b) $\gamma_b = 1.5$, n = 2, (c) $\gamma_b = 10$, n = 1, and several values of parameter $\eta$.